Development of Subscale Fast Cookoff Test

Alice I. Atwood[1], Kenneth J. Wilson[2], Travis S. Laker[3], and Ephraim B. Washburn[4]
Naval Air Warfare Center Weapons Division, China Lake, CA, 93555

A propane-fueled combustor was built to support the development of an alternate to the external fire test currently required for final Hazards Classification (HC). The device has the capability to provide a controlled heat flux environment of 40-400 kW/m^2 (12,600-126,000 Btu/hr/ft^2). This results in a repeatable and quantifiable environment for the evaluation of the fast cook-off response of an ordnance item.

Nomenclature

q''	=	heat flux
h	=	heat transfer coefficient
T	=	temperature
k	=	thermal conductivity
D	=	diameter
Nu	=	Nusselt number
Re	=	Reynolds number
Pr	=	Prandtl number
μ	=	viscosity
σ	=	Stefan-Boltzmann constant
ε	=	emissivity

I. Introduction

THIS paper presents a report on the design and development of a controlled heat flux combustor in support of a larger task aimed at the development of a sub-scale alternate test protocol to the external fire test currently required for final Hazards Classification (HC) of an ordnance system. The specific goal of this part of the task was to design a thermal stimulus that could be controlled and still deliver the flux levels encountered in a liquid fuel fire of the type related to transportation and storage.

In the United States, all ordnance systems must be hazard classified. TB 700-2 is the documentation that is used for the hazards classification process.[1] The hazards classification procedures have been harmonized with both the UN Test and Criteria Manual for UN Series 1.1 through 1.4[2] and for the appropriate NATO STANAG. As described in TB 700-2, the ordnance system is hazard classified by performance of the system level tests listed in Table 1, or by performance of an approved alternate test, or by performance of an alternate plan that has received the approval of the appropriate service hazard classifier. Once the alternate tests have been performed, the results must be approved by the service hazard classifier and the Department of Defense Explosive Safety Board (DDESB).

Table 1. HD 1.1 - 1.4 assignment tests.

Single package
Sympathetic reaction
Liquid fuel/external fire

Currently TB 700-2 contains three tests for explosive shock stimuli that have been approved as alternates for the system level tests for single package and sympathetic reaction, but there are no approved alternate tests for the liquid-fuel/external-fire test. The initial cost of a full-scale asset, the potential hazards associated with conducting the test, and the amount of real estate required for an appropriate test site are some of the difficulties in performing

[1] Physical Scientist, Energetics Research Division, 1 Administration Circle
[2] Aerospace Engineer, Energetics Research Division, 1 Administration Circle, Member AIAA
[3] Mechanical Engineer, Energetics Research Division, 1 Administration Circle, Member AIAA
[4] Chemical Engineer, Energetics Research Division, 1 Administration Circle

Report Documentation Page

Form Approved
OMB No. 0704-0188

1. REPORT DATE	2. REPORT TYPE	3. DATES COVERED
14 NOV 2006	**N/A**	**-**

4. TITLE AND SUBTITLE	5a. CONTRACT NUMBER
Development of Subscale Fast Cookoff Test	5b. GRANT NUMBER
	5c. PROGRAM ELEMENT NUMBER
6. AUTHOR(S)	5d. PROJECT NUMBER
	5e. TASK NUMBER
	5f. WORK UNIT NUMBER
7. PERFORMING ORGANIZATION NAME(S) AND ADDRESS(ES) **Naval Air Warfare Center Weapons Division, China Lake, CA, 93555**	8. PERFORMING ORGANIZATION REPORT NUMBER
9. SPONSORING/MONITORING AGENCY NAME(S) AND ADDRESS(ES)	10. SPONSOR/MONITOR'S ACRONYM(S)
	11. SPONSOR/MONITOR'S REPORT NUMBER(S)

12. DISTRIBUTION/AVAILABILITY STATEMENT
Approved for public release, distribution unlimited

13. SUPPLEMENTARY NOTES
See also ADM202095, Proceedings of the 2006 AIAA Missile Sciences Conference Held in Monterey, California on 14-16 November 2006.

14. ABSTRACT

15. SUBJECT TERMS

16. SECURITY CLASSIFICATION OF:			17. LIMITATION OF ABSTRACT	18. NUMBER OF PAGES	19a. NAME OF RESPONSIBLE PERSON
a. REPORT	b. ABSTRACT	c. THIS PAGE			
unclassified	**unclassified**	**unclassified**	**SAR**	**10**	

the external fire test on large solid rocket motors. Since only one trial is required, the statistical significance of the test is questionable.

DDESB and the Joint Hazards Classifiers (JHC) have recognized the need for alternatives to the external fire test. They have supported the development of a technology base to achieve viable alternate tests.

II. Approach

A critical part of any alternate approach for thermal hazard classification is a heat source that can provide the appropriate heat flux levels over the appropriate time intervals in a controllable and reproducible manner. A hierarchical or top down approach has been used in the design and development of the controlled heat flux device.[3,4] A top down diagram related to the development of the current device is shown in Figure 1.

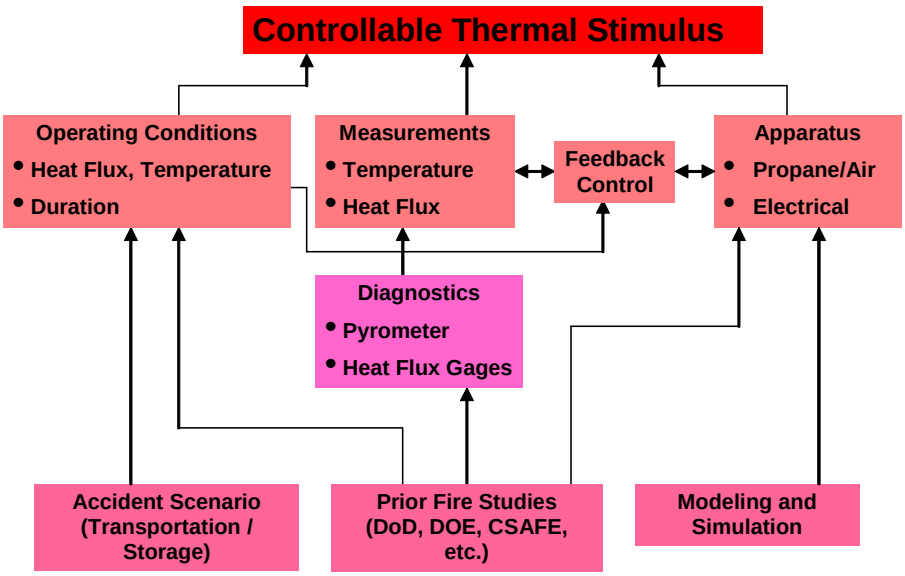

Figure 1. Diagram for development of controllable thermal stimulus.

The derivation of the thermal-heat-flux requirement was initiated with a review of accident data from the Department of Defense Explosive System Safety Mishap database, ESSM. Those findings were reported in the 31st United States Department of Defense Explosives Safety Seminar of 2004.[5] Data from related fire studies throughout the DOD, DOE and academia were also utilized, particularly, the ASCII sponsored work of the CSAFE Program.[6]

The results of these investigations indicated that thermal flux levels of 20 to 200 kW/m^2 (6,300 to 63,000 Btu/hr/ft^2) could be obtained during a thermal event, with the potential for that range of flux levels to exist simultaneously in the fire.[7,8] These data validated the conclusion that a controllable flux device was needed for these studies to be effective. The device must also be tunable to allow for a range of heat flux values to be obtained. For the current effort, flux levels of 50, 75, and 100 kW/m^2 (16,000, 24,000, and 32,000 Btu/hr/ft^2) have been selected for study. It should be noted that in the case of a fast cookoff event, the lower flux levels and longer thermal soak times may represent the most violent reactions, due to the involvement of a larger amount of energetic material in the cookoff reaction.

III. Apparatus

The physical nature of a fuel-fire is very difficult to quantify and measure. Understanding how the heat flux is coupled from the fuel fire flames to a specific target is important to experimental and computational modeling efforts in this area. The controlled heat flux device was conceived to provide the basis for a small-scale fuel-fire test for hazard classification and to probe the underlying physical response to the external fire test in a controlled manner. Options that were considered for the test device were electric resistive heating, radiative heating, and propane/air. All of these devices have positive and negative features and are under development at a number of research facilities.

The electric resistive heating approach was rejected because of the concerns that an appropriate heating rate could not be achieved and that the need for contact with the test vehicle might interfere with the response of the item relative to violence. Radiative heating was also rejected due to the overall cost of the system. The propane-fueled combustor was selected due to its ease of construction at a reasonable cost. The apparatus will allow for the study of both convective and radiative heating.

The apparatus is intended to apply a uniform and constant heat flux level to a small-scale sample so as to simulate the thermal penetration of heat flux experienced by a full-scale device in a fuel fire. The device seeks to be controllable, tunable, and variable in its rate of heat flux application. It has both reusable and expendable sections and provides a method of assessing the reaction violence with fragmentation of a portion of the test section.

A. Design

The schematic of Figure 2 shows the major components of the combustion device and how those components provide the means necessary for the combustor to operate. Air enters the combustion chamber via a duct at a flow rate determined by the required operating heat flux conditions. Fuel is injected at a location in the air duct so that the fuel can be mixed with the air, which will provide a flammable mixture. This mixture is then ignited in the combustion chamber, at which time the fuel is consumed in the reaction region, generating high-temperature gas products. The combustion chamber has an inside diameter that is larger than the air duct. The change in area from the smaller air duct to the larger combustion chamber allows flame stabilization for the reaction region. The amount of fuel and air introduced into the chamber controls the gas temperature and therefore the heat flux.

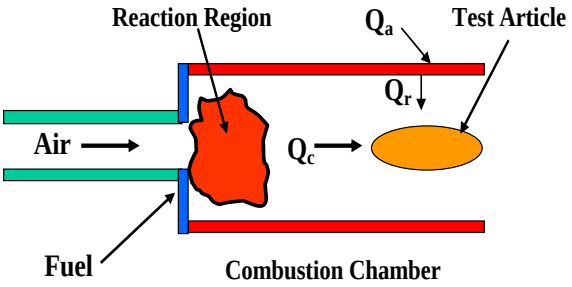

Figure 2. Basic schematic of controlled heat flux device.

The test article contains energetic material that will be subjected to a controlled heat flux for evaluation. The heat flux is generated by two components in the combustion chamber. One component of the heat flux is the convective (q_{conv}") high temperature gases from the combustion products, while the second component is from radiation (q_{rad}") generated from the high temperature wall surface. The wall surface can be heated to the required temperature by the high temperature gases of the reaction region, or can be augmented by introducing additional heat (q_{add}") to certain areas of the combustor wall.

The nonexpendable portion of the controlled heat flux combustor is shown in Figure 3. A five horsepower fan motor (Figure 4) delivers air through a 12 cm (5.0 inch) diameter stainless steel air duct. The fan, when driven at 3870 RPM, will deliver a mass flow rate of ~0.5 kg/sec (l.0 lb/sec). Fuel is introduced through an aluminum manifold located at the end of the tube via eight injectors as shown in Figure 5. An array of eight injectors was selected to provide uniform fuel distribution. Liquid propane injection is shown in Figure 6.

The fuel/air mixture expands into a 0.46 m (18 inch) diameter stainless steel combustion chamber. The non-expendable portion of the chamber is approximately 2 meters (6 feet) in length. An additional 2 meters (6 feet) of combustion chamber represents the expendable portion of the test apparatus and will act as a witness tube should fragmentation occur during the experiment.

B. Challenges

To provide the necessary heat flux in the present combustor, it was decided to supply the propane fuel as a liquid in order to generate the 1.0 MW (3.4 MBTU/hr) of power. With an approximate flow rate of 3.0 liters/min (1500 grams/min at 73 F^o), a device capable of generating 10 kW (34000 BTU/hr) of power would be required to vaporize the liquid if gaseous propane had been chosen for this device. Another consideration is that the resulting expansion from the liquid to gas phase would also need much larger plumbing for the gaseous injection into the combustor. The volumetric increase of propane from liquid-to-gas is a factor of 254.

The vapor pressure of the stored propane should be adequate for the fuel delivery to the combustor at ambient pressure. At 0º C (32º F), the pressure is 370 kPa (54 psig) and at 50º C (122º F), the pressure is 1590 kPa (230 psig). However, tests conducted at various times of the year, when outside temperatures varied from 0º to 50º C (32º to 122º F), concluded that the fuel system could not operate reliably at the low vapor pressure. Because the fuel delivery pressure must be reduced from the vapor pressure in the storage tank to the ambient pressure in the combustor, a phase change occurs at the fuel-metering orifice resulting in a 2-phase flow in the fuel distribution manifold. The resulting expansion of the gas phase created a very unsteady and unreliable flow rate in the injection system. A solution is currently being tested with a redesigned regulation orifice and distribution manifold. This

system utilizes a fixed orifice for the pressure reduction and mass flow control. The placement is critical due to the requirement that an immediate volume increase be present to accommodate the partial expansion of the gas phase. Since propane is a refrigerant, those characteristics are used to condense the gas portion of the 2-phase mixture back to liquid only. This is accomplished by utilizing the latent heat of vaporization provided during the partial expansion process. The temperature in the aluminum distribution manifold is now lowered enough by this cooling that the gas can condense because the local vapor pressure is reduced.

While the present design does not allow for fuel adjustment during a test, it will provide enough information to construct a device that will have controllability to maintain a desired heat flux condition.

Figure 3. Nonexpendable portion of the controlled heat flux combustor.

Figure 4. Controlled heat flux combustor blower fan.

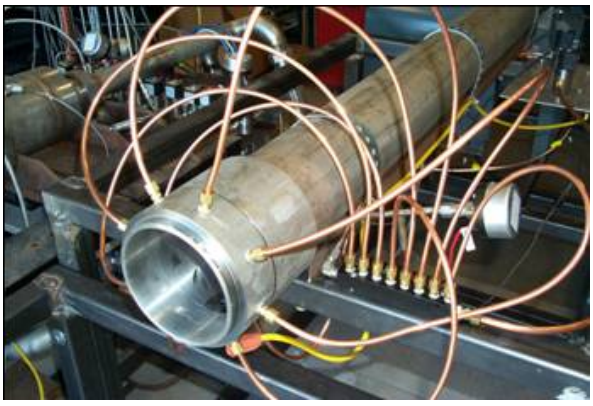

Figure 5. Liquid propane injection.

Figure 6. Liquid propane injection.

IV. Calculations

A. Simple Engineering Analysis Calculations

Heat fluxes into objects submersed in pool fires range from 40 kW/m^2 to 400 kW/m^2 (12,600-126,000 Btu/hr/ft^2). Using this range of heat fluxes, some simple calculations were performed to determine the feasibility of the proposed controllable heat flux device. The convective heat flux into the test article was estimated using Equations 1 - 3.[9]

$$q''_{conv} = h\left(T_{air} - T_{article}\right) \tag{1}$$

$$h = \left(k/D\right)Nu \tag{2}$$

$$Nu = 0.027 Re_D^{\,4/5} Pr_D^{\,1/3} \left(\mu/\mu_s\right)^{0.14} \tag{3}$$

Bounding calculations where done with various incoming gas temperatures (1000 K to 1500 K, 1340º F to 2240º F) and velocities (7.6 m/sec to 91 m/sec, 25 ft/sec to 300 ft/sec). Heat fluxes of 16 kW/m^2 to 170 kW/m^2 (5,000 Btu/hr/ft^2 to 53,900 Btu/hr/ft^2) were calculated over the design space. These results were presented to the experimentalist. They commented that the temperature range was achievable. However, one of the constraints of the design was cost and portability. The desire was to provide the air with a relatively inexpensive fan and not use compressed air. They stipulated that the air mass flow rate should be around 0.45 kg/sec (1.0 lb/sec) and not exceed 0.90 kg/sec (2.0 lb/sec). This corresponded with a velocity upper limit of ~27 m/sec (~89 ft/sec). This interchange with the experimentalist provided a more realistic upper bound for the convective heat transfer of 65 kW/m^2 (21,000 Btu/hr/ft^2). The calculated heat flux at the desired mass flow of 0.45 kg/sec (1.0 lb/sec) ranged from 38 kW/m^2 to 20 kW/m^2 (12,000 Btu/hr/ft^2 to 6,300 Btu/hr/ft^2)with air temperatures of 1500 K to 1000 K (2240º F to 1340º F).

Realizing that radiation will be a major form of energy exchange in the device, simple bounding radiation heat flux calculations into the test article were performed. Equation 4[9] was used to determine radiative heat flux exchange between concentric cylinders.

$$q''_{rad} = \frac{\sigma\left(T_{wall}^4 - T_{article}^4\right)}{\frac{1}{\varepsilon_{article}} + \frac{1-\varepsilon_{wall}}{\varepsilon_{wall}}\left(\frac{D_{article}}{D_{wall}}\right)} \tag{4}$$

Stainless steel was the material to be used for the outer wall cylinder. The emissivity of hot stainless steel ranges from 0.5 to 0.8 depending on the level of oxidation. The emissivity of the test article could have a similar range for metal cases or higher for composite cases. Using the same temperature range for the outer wall as the hot incoming gas (1500 K to 1000 K, 2240º F to 1340º F) and wall emissivity of 0.65 and article emissivity of 0.8, the radiative heat flux was calculated to be 190 kW/m^2 to 30 kW/m^2 (60,200 Btu/hr/ft^2 to 9,500 Btu/hr/ft^2). In the calculations, using the low temperatures the contribution of radiation and convection to the heat flux into the test article are similar. Since the radiative heat flux is a function of the wall temperature to the fourth power, the contribution of radiation to the incoming heat flux increased much faster than that of convection. Using the upper temperature range, the radiative heat flux was calculated to be 5 times that of convection.

The initial heat flux calculations were important in that they showed that the device could deliver the desired heat flux to a test article. They also showed that there could be a significant amount of control of the heat flux into a test article by changing the incoming mass flow and temperature. These straightforward and easily performed calculations established feasibility and the design of the device was continued.

B. Iterative High-Fidelity Design Calculations

The simple engineering analysis effectively bounded and constrained the problem and allowed an initial concept to be generated. The next step in the computational portion of the design process was the relaxation of the assumptions and generalities (geometry and physics) that are inherent in the simple engineering calculations. The added level of detail and improved accuracy provided necessary information in design of the actual design prototype. Numerical heat transfer methods were used to predict the response of the test article. Computational fluid dynamics (CFD) tools were used to estimate the flow and heat transfer around the test article within the combustor. Each of these areas will be discussed briefly.

1. Numerical Heat Transfer Modeling

During the initial phases of this project, NAWCWD China Lake created a transient thermal penetration model of a thermally protected composite-cased rocket motor. A two-dimensional axi-symmetric model was created using MPCoyote,[10,11] a thermal analysis software package from Sandia National Laboratory. The model used temperature dependent properties for the primary materials and tracked the extent of thermal penetration as a function of time. Figure 7 is a temperature versus time plot showing the thermal penetration of a composite cased rocket motor at a specified heat flux level. While this model neglected charring and ablation of the thermal protection layers and the graphite-epoxy composite case, it was useful in predicting the characteristic thermal profile and estimated the order of magnitude of the thermal penetration time. The experimentalist used the thermal penetration time information to determine the required size of the fuel source. The resulting thermal traces indicated a strong dependence on the thermal properties of the outer layers of the case system and showed that the appropriate physical mechanisms were required for these materials.

It is necessary for any small-scale test article to represent the full-scale item as closely as possible. The experimental design of the small-scale article showed that when the thickness of the case wall (composite case, liner, and insulation) remained fixed and the overall diameter decreased, the test article case retained an excessive amount

of strength. It was also unclear how the reduction in case thickness of the test article would affect the thermal response. These two competing system properties required detailed analysis and consideration. The detailed

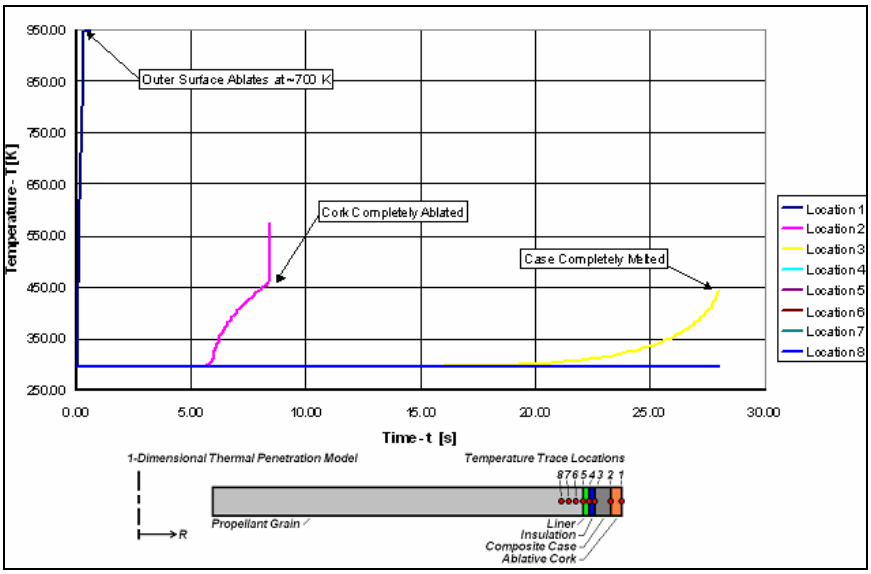

Figure 7. Temperature versus time profiles for a large diameter composite rocket motor exposed to an exterior surface heat flux of $q'' = 100{,}000$ W/m^2.

numerical heat transfer model was used to address the associated thermal issues.

The effect of the diameter of the propellant grain on the thermal penetration was analyzed using the numerical heat transfer model. To address this issue, the numerical heat transfer model of the full-scale rocket motor was compared to sub-scale analog models. The subscale models consisted of 0.454 m (17.8 inches), 0.170 m (6.69

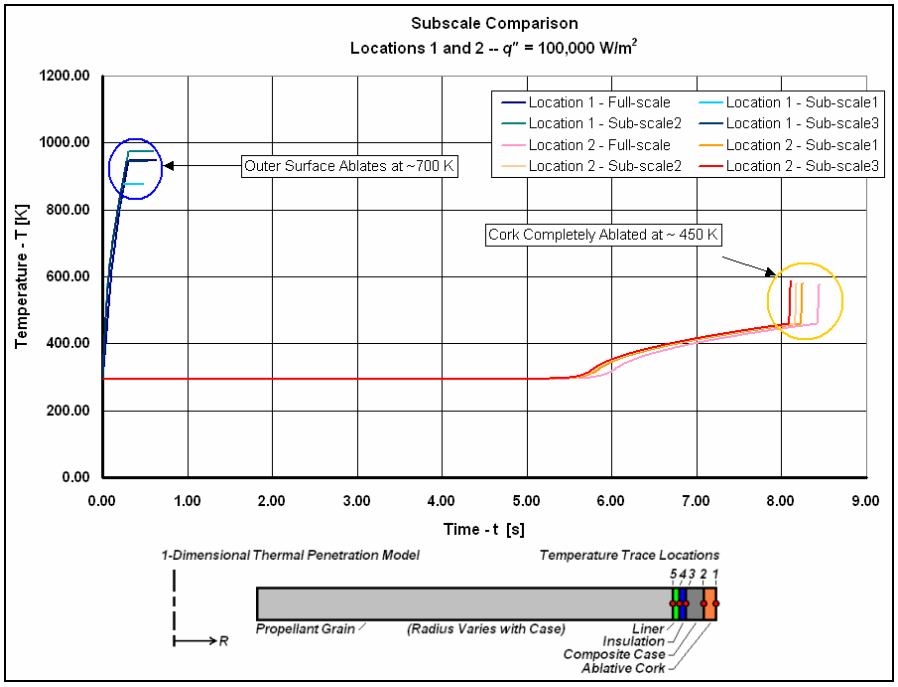

Figure 8. Thermal penetration profiles for full- and sub-scale motor models.

inches), and 0.061 m (2.40 inches) diameter-propellant-grains motors. These subscale models employed the same thickness dimensions for the case materials, but varied the diameter of the propellant grain. Figure 8 displays the

time dependent thermal traces of the full- and sub-scale models. The agreement of the curves in Figure 8 indicates that the predominant thermal effects occur in the case/insulation/liner materials and not in the propellant grain. From this result, it was concluded that a small-scale alternate test for the external fuel fire hazards classification test was feasible for large diameter, composite cased rocket motors.

2. Computational Fluid Dynamics Simulations

The engineering calculations of the heat flux into the test article gave bounding values, but higher fidelity calculations were desired to further refine the actual magnitude of the possible heat fluxes into the test article. The commercial CFD software Fluent[12] was used to determine the contribution of convection and radiation to the overall heat flux. The configuration used in the calculations is given in Figure 9.

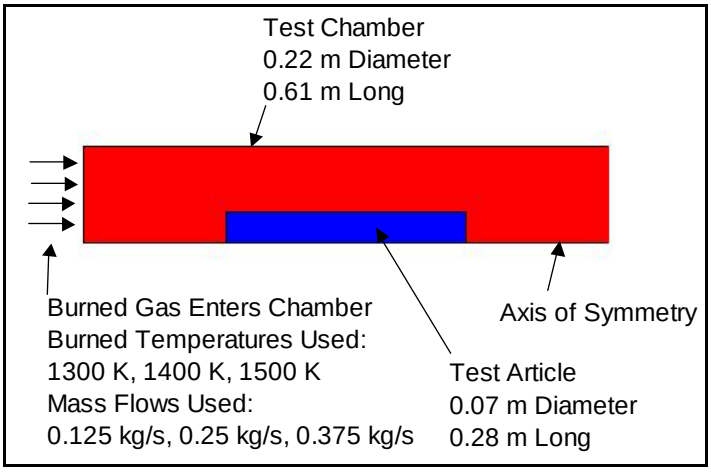

Figure 9. Computational setup for sizing calculations.

The calculations were done at two different test chamber diameters, three inlet gas temperatures, and three mass flows. The results are shown in Figure 10. The results demonstrated that the device could deliver almost an order of magnitude of different heat fluxes to the test article depending on the mass flow and the gas temperature. The results show that the radiative component of the incoming heat flux is the greatest.

It is important to note that the high fidelity calculation compare reasonable well with the simple engineering calculations. For the convective heat flux, the Fluent calculations and the simple equation calculations were within 25% - 50% of each other. This agreement between the separate calculations gives additional confidence to the results. The radiation calculations had the same trend, but the magnitude of the simple radiation calculation was up to 2 times that of the value calculated by Fluent. This was expected since the approximations were greatest for the simple radiative heat flux calculations and they were supposed to give an upper bound. This shows the importance of running the high fidelity calculations to refine the results.

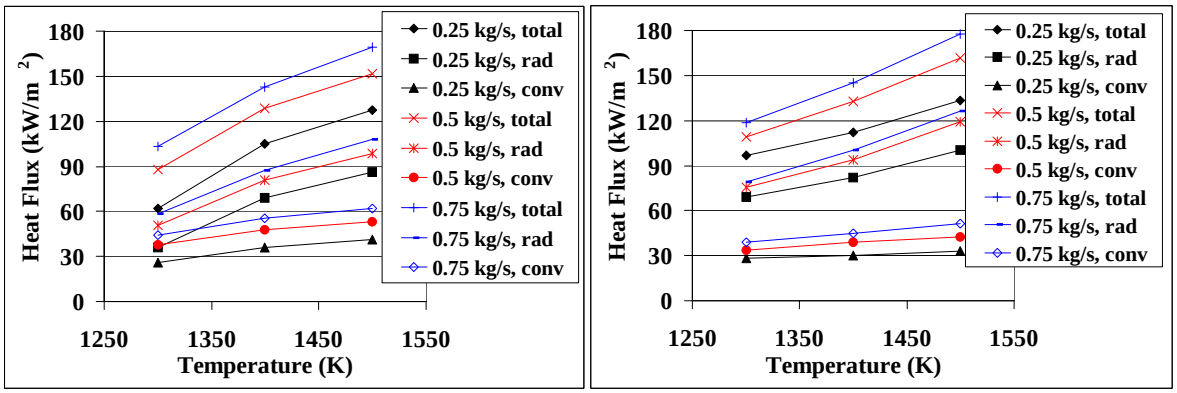

Figure 10. Heat Flux into Test Article vs. Temperature of Gas with a Chamber Diameter of 0.3 m (left graph) and 0.46 m (right graph).

Another advantage of high fidelity modeling is the additional information acquired. For overall heat flux, the simple and high fidelity model are comparable. However, the simple model gives no information on the flow structure or temperature distribution within the device. An example of the advantage of having this information is given in designing the fuel injectors. The experimentalist wanted to design the inlet diameter so the propane would sufficiently penetrate the chamber, but not cross the line of symmetry. It was suggested that 0.064 cm (0.025 inches) would work. Since the geometry and flow field were already in place, a drop model was added to investigate droplet dispersion. Figure 11 shows the propane droplet concentrations for injector openings of 0.25 cm (0.10 inches), 0.13 cm (0.05 inches), and 0.064 cm (0.025 inches). The 0.25 cm (0.10 inches) diameter injector

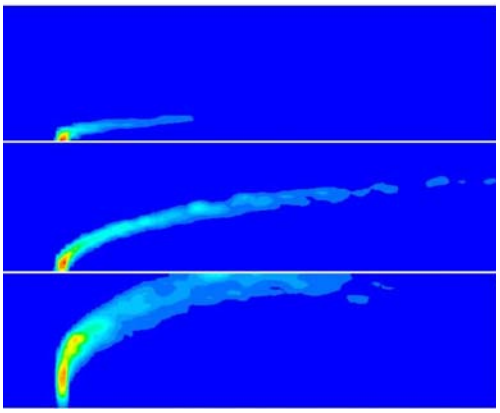

Figure 11. Droplet Concentration Profiles for Three Injector Diameters: 0.25 cm (top), 0.13 cm (middle), 0.064 cm (bottom).

Figure 12. Controlled heat flux combustor operating at 1400ºC.

shown on the top did not penetrate enough of the test chamber, while the 0.064 cm (0.025 inches) diameter injector had too large of a penetration. The 0.13 cm (0.05 inches) diameter injector was chosen as the best option.

V. Results

The expendable combustion chamber was omitted for the initial controlled flux testing. Eight Type K thermocouples were located along the exterior wall of the combustion chamber ~ 0.23 m (9.0 inches) apart. These thermocouples were used to evaluate the position of flame attachment in the combustor and to gain insight into the level of heat loss to the combustor wall. An additional type B thermocouple in a ceramic housing was located at the exhaust as shown in Figure 12. The external wall temperatures are compared to the exhaust temperature for a typical run in Figure 13.

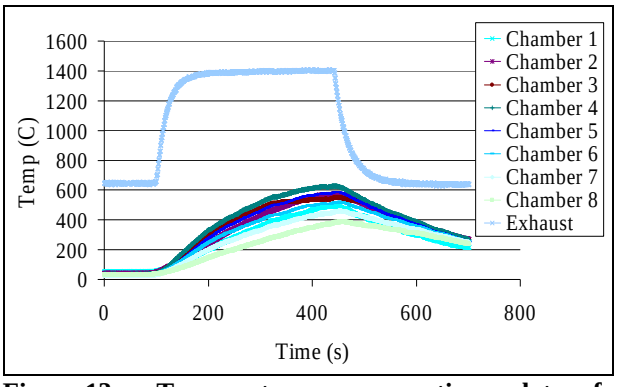

Figure 13. Temperature versus time data for controlled flux combustor operation.

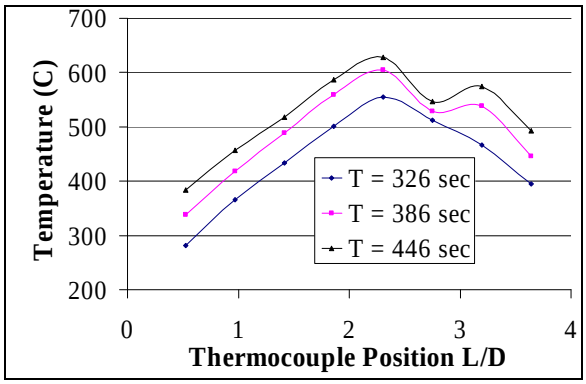

Figure 14. Temperature of wall mounted thermocouples.

This test was run for approximately 5 minutes at a temperature (1400º C, 2550º F) to check out the maximum operating capabilities of the device. This time duration was long enough to verify a uniform gas temperature and to evaluate flame location without potentially damaging the combustion chamber pipe. The exhaust temperature in Figure 13 shows a time lag to steady state conditions of 100 seconds. The observed lag is due to the slow response of the type B thermocouple used for this measurement. The thermocouple was an industrial version with a large massive protective ceramic enclosure that would have a very slow response time. The temperature steady state condition is most likely several seconds and will be measured later with a fast response 0.025 cm (10 mil) thermocouple. An important consideration for thermal lag of the system would be the time to heat the mass of the walls to provide the radiation component of the heat flux. This will also be measured later by a calibration device.

External temperatures of the wall-mounted thermocouples at three different times are given in Figure 14.

VI. Future Plans

Figure 15 gives a concept of a calibration tool that is currently being constructed. The calibration device will have the same exterior shape as the test article. The calibration device (and test article) will be fitted with a flow diverter nose cone, which will provide a uniform heat flux along the cylindrical wall of the device. The calculations indicate that a 25 cm (10 inches) flow diverter is needed for uniform thermal flux. The cylindrical portion of the device is being fitted with six water-cooled Vatell™ heat flux microsensors.[13] These sensors were selected because they will operate in a cross flow condition. The cylinder will be water cooled to allow the microsensors to function properly over the entire temperature range. The mounting cylinder will be 12 cm (5.0 inches) in diameter, as it was determined that the heat flux microsensors could not be mounted in a smaller diameter. Overall length of the cylindrical portion of the calibration unit is 25 cm (10 inches). The calibration tool is being manufactured and calibration at the test article location will commence upon its completion. Once the calibration of the system is complete the controlled heat flux device will be relocated to the remote test site where the evaluation of energetic materials will begin.

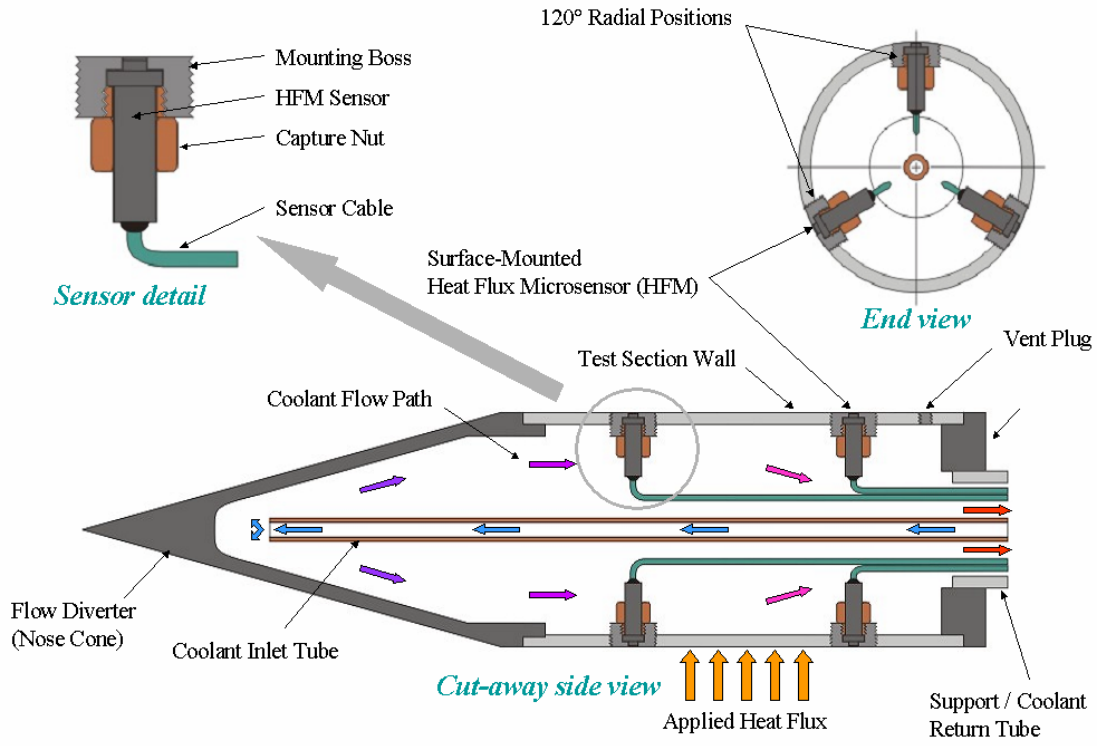

Figure 15. Concept of the test vehicle calibration tool.

The controlled heat device will be used to provide the necessary thermal data on the mechanistic variables that are associated with cook-off reaction violence. The ability to control the heat flux will result in data that are reproducible and of sufficient fidelity to be input into the analytical tools currently being used to design a viable alternate thermal test.

VII. Conclusion

A controllable heat flux device has been designed and assembled. The test fixture was constructed in support of an ongoing effort to develop an alternate test protocol to the external fire test required for final hazard classification of ordnance systems. The device will be used to examine the effects of thermal flux on the response of an ordnance device in a controlled environment.

Modeling and simulation tools were used to design the apparatus and provided aid in its construction. The device consists of a modular design so that modifications can easily be made as needed. The modular construction allows for transportation of the device to remote test locations.

The controlled heat flux combustor is constructed from parts that are readily available, and is repairable when damage occurs. A portion of the combustor is designed to act as a witness tube for evaluation of reaction violence.

No single part of the controlled heat flux device exceeds $1000 in cost. The diameter of the chamber is 46 cm (18 inches) and should accommodate a test article up to 23 cm (9 inches) in diameter. The length of the test article is dependent upon the ability to support the device and the amount of heat loss encountered in the increased chamber length.

The controlled heat flux combustor operates with liquid propane, a readily available fuel with a high energy density. The fuel is self pressurized. The combustor does not require high-pressure air for mass flow rates up to 0.5 kg/sec (1 lb/sec). The heat flux is a combination of radiation emitted from the chamber walls and convection from the 3.0 m/sec (9.8 ft/sec) gas flow within the combustor. Adjusting the total mass flow rate and/or the temperature of the mixture controls the power level of the test fixture.

Acknowledgments

This work was performed under funding from US Air Force through the Air Force Research Laboratory and under funding from the Department of Defense Explosive Safety Board.

References

[1] TB 700.2 NAVSEAINST 8020.5C, to 11A-1-47, DLAR 8220.1, Joint Technical Bulletin, "Department of Defense Ammunition and Explosives Hazard Classification Procedures," final draft, May 2004.

[2] Recommendations on the Transport of Dangerous Goods, Tests and Criteria, ST/SG/AC.10/11 latest revision, United Nations publication, New York, New York.

[3] Oberkampf, W. L., and Trucano, T. G., "Validation Methodology in Computational Fluid Dynamics," AIAA Paper 2000-2549, Fluids 2000, June 2000.

[4] Oberkampf, W.L., Trucano, T.G., and Hirsh, C., "Verification, Validation, and Predictive Capability in Computational Engineering and Physics," Sandia National Laboratories, SAND2003-3769, Albuquerque, New Mexico, 2003.

[5] Rattanapote, M.K., Atwood, A.I., and Covino, J., "A Survey of Transportation and Storage Accidents Involved in Thermal Events," *Proceedings of 31st United States Department of Defense Explosives Safety Seminar*, CPIA, Laurel, Maryland, August 2005.

[6] Spinti, J.P., Eddings, E.G., Smith, P.J., and Sarofim, A.F., "Heat Transfer to Containers in Pool Fires," *Transport Phenomena in Fires*, WIT Press, Southampton, UK, 2006.

[7] Kramer, M.A., Greiner, M., Koski., J.A., and Lopez., C. and Sou-Anttila, A., "Measurements of Heat Transfer to a Massive Cylindrical Calorimeter Engulfed in a Circular Pool Fire," *Journal of Heat Transfer*, Vol. 125, 2003, pp. 110-117.

[8] Kramer, M.A., Greiner, M., Koski., J.A., and Lopez., C. "Uncertainty of Heat Transfer Measurements in and Engulfing Pool Fire," *Thermal Measurements: The Foundation of Fire Standards*, ASTM STP 1427, American Society for Testing and Materials, West Conshohocken, Pennsylvania, 2001.

[9] Incropera, F.P., and DeWitt, D.P, *Fundamentals of Heat and Mass Transfer*, 4th ed., John Wiley & Sons, New York, NY, 1996.

[10] Gartling, D.K., Hogan, R.E., and Glass, M.W., "COYOTE – A Finite Element Computer Program for Nonlinear Heat Conduction Problems, Part I – Theoretical Background," Sandia National Laboratories, SAND94-1173 Unlimited Release, Albuquerque, NM, Jan 2003.

[11] Gartling, D.K., Hogan, R.E., and Glass, M.W., "COYOTE – A Finite Element Computer Program for Nonlinear Heat Conduction Problems, Part II – User's Manual," Sandia National Laboratories, SAND94-1179 Unlimited Release, Albuquerque, NM, Jan 2003.

[12] Fluent, CFD Software Package, Ver. 6.2, Lebanon, NH, 2005.

[13] Diller. T. E., "Advances in Heat Flux Measurements," *Advances in Heat Transfer*, Vol. 23, 1993, pp. 273-367.